ARTICLE

Phase Separation as a Tool to Control Dispersion of Multiwall Carbon Nanotubes in Polymeric Blends

Suryasarathi Bose,[†] Ceren Özdilek,[†] Jan Leys,[‡] Jin Won Seo,[§] Michael Wübbenhorst,[‡] Jan Vermant,[†] and Paula Moldenaers*,[†]

Department of Chemical Engineering and Leuven Materials Research Center, Katholieke Universiteit Leuven, Willem de Croylaan 46, B-3001, Leuven, Belgium, Department of Physics and Astronomy, Celestijnenlaan 200D, Katholieke Universiteit Leuven, B-3001, Leuven, Belgium, and Department of Metallurgy and Materials Engineering, Kasteelpark Arenberg 44, Katholieke Universiteit Leuven, B-3001, Leuven, Belgium

ABSTRACT Conducting polymeric materials with stable phase microstructures have a range of potential applications. In this work, it is investigated whether phase separation in polymer blends can be used as a tool to create well dispersed conducting filler rich domains in 3D with controlled morphology, potentially resulting in more effective percolation. The effect of amine functionalized multiwall carbon nanotubes (NH_2-MWCNTs) on the thermally induced phase separation processes in poly[(α-methyl styrene)-*co*-acrylonitrile]/poly(methyl methacrylate) (PαMSAN/PMMA) blends was monitored by melt rheology, conductivity spectroscopy, and microscopic techniques. Electron microscopic images revealed that the phase separation resulted in a heterogeneous distribution of NH_2-MWCNTs in the blends. The migration of NH_2-MWCNTs is controlled by the thermodynamic forces that drive phase separation and led to an increase in their local concentration in a specific phase resulting in percolative "network-like" structure. Conductivity spectroscopy measurements demonstrated that the blends with 2 wt % NH_2-MWCNTs that showed insulating properties for a one phasic system revealed highly conducting material in the melt state (two phasic) as a result of phase separation. By quenching this morphology, a highly conducting material with controlled dispersion of MWCNTs can be achieved. Furthermore, the role of NH_2-MWCNTs in stabilizing the PMMA droplets against flow induced coalescence in 85/15 PαMSAN/PMMA blends was also established for the first time. It was observed that at a typical loading of 1.25 wt % NH_2-MWCNTs the coalescence was completely suppressed on a practical time scale.

KEYWORDS: phase separation • multiwall carbon nanotubes • percolation • morphology • electrical conductivity • coalescence suppression

1. INTRODUCTION

The phase separation in polymer blends can proceed by two mechanisms: nucleation and growth on the one hand and spinodal decomposition on the other. The resulting morphology of the blends can be either of the matrix-droplet or of cocontinuous type and is not necessarily linked with the mechanism of phase separation. It is also known that the coarsening of matrix-droplet morphology is typically a slow process whereas interconnected structures coarsen rather rapidly (1). As the performance-properties of polymer blends are tightly related to the morphology, various strategies have been developed to achieve fine phase morphologies during processing. However, it is difficult to stabilize the morphology during processing as the thermodynamic driving force causes the droplets to coalesce. In this context, the use of block copolymers at the interface has been proven to be a successful strategy in suppressing coalescence. Recently, the use of nanoparticles such as carbon black (CB), clay, silica, etc. to stabilize the phase morphology of polymer blends has been extensively reported (for a review see ref 2).

The discovery of carbon nanotubes (CNTs) has paved the way for designing novel materials in view of their extraordinary combination of electrical, mechanical, and thermal properties (3). It has been realized that the "network-like" structure of CNTs in a polymer matrix reduces the percolation concentration to a significant extent and improves the bulk electrical conductivity of the system. In the case of binary polymer blends, the localization of CNTs with respect to either phase dictates the percolation concentration. In addition, recent reports have also shown the potential of CNTs in refining the phase morphology of binary polymer blends (4, 5). In this context, the effect of the localization of filler either at the interface or in a specific phase is not yet fully resolved.

The idea behind the use of nano particles at the interface of immiscible polymer blends to stabilize the phase morphology stems from the utilization of colloidal particles to stabilize emulsions resulting in "Pickering" emulsions (6) and

* Corresponding author. Fax: +32 16 322991. E-mail: paula.moldenaers@cit.kuleuven.be.

Received for review November 19, 2009 and accepted February 16, 2010

[†] Department of Chemical Engineering and Leuven Materials Research Center, Katholieke Universiteit Leuven.

[‡] Department of Physics and Astronomy, Katholieke Universiteit Leuven.

[§] Department of Metallurgy and Materials Engineering, Katholieke Universiteit Leuven.

DOI: 10.1021/am9008067

Published on Web 02/25/2010

Bijels (7). For example, Vermant et al. (8) showed that localization of nanosilica at the interface of polydimethylsiloxane/polyisobutene blends can slow down the coalescence of polyisobutene droplets on a practical time scale for concentrations above 0.5 wt % and can completely suppress it at 1 wt % in blends with 30 wt % dispersed phase. The localization of filler in a specific phase or at the interface in an immiscible polymer blend is governed by thermodynamic and kinetic factors. For example, it was demonstrated that CB particles accumulate at the interface of polyethylene/polystyrene (PE/PS) blends for a period of time that strongly depends on the rheology of the blends during processing. Such thermodynamically controlled localization of CB particles dramatically reduced the percolation concentration in immiscible blends and also stabilized the phase morphology (9).

The rationale behind the present work is to investigate whether phase separation processes in polymer blends can be used as a tool to create well dispersed multiwall carbon nanotubes (MWCNTs) rich domains in 3D, potentially resulting in effective percolation. For this purpose, lower critical solution temperature (LCST) type blends of poly[(α-methyl styrene)-*co*-acrylonitrile]/poly(methyl methacrylate) (PαMSAN/PMMA) have been selected as a model system and an industrially viable route for processing them (melt mixing). It is interesting to monitor the morphology development of these blends with time and temperature as the phase separation may influence the distribution of MWCNTs in the blends. In addition, the potential of MWCNTs for stabilizing the droplets against flow induced coalescence has also been investigated. Conductivity spectroscopy measurements and electron microscopic analysis have been performed to gain in depth insight into the state of dispersion of MWCNTs during phase separation in the blends.

2. EXPERIMENTAL SECTION

2.1. Materials. Both PαMSAN (Luran KR2556) and PMMA (Lucryl G77) were obtained from BASF. An overview of the characteristics of these polymers and of the phase behavior of the blends has been extensively discussed in ref 10. The amine functionalized MWCNTs (NH_2-MWCNTs, NC3152) were obtained from Nanocyl (Belgium) (11). The electrical conductivity of MWCNTs has been reported to be on the order of 10^4 S/cm (12).

2.2. Processing. Two sets of blends, 85/15 and 15/85 PαMSAN/PMMA, were prepared with or without NH_2-MWCNTs by melt mixing, using a 15 cm^3 DSM microcompounder at 190 °C with a rotational speed of 60 rpm for 20 min. The mixing was performed under nitrogen atmosphere in order to prevent oxidative degradation. The cloud point temperatures of 85/15 and 15/85 PαMSAN/PMMA blends were reported to be 190 °C and ~155 °C, respectively (10). Hence, the extrudate strands were subsequently compression molded at 160 °C.

2.3. Characterization. The viscoelastic properties of the components and the blends were studied using an AR2000ex stress-controlled rheometer (TA Instruments) with parallel plate geometry (25 mm in diameter and 1 mm gap distance) under N_2 atmosphere. Time-sweep measurements using a fixed frequency (0.1 rad/s) and strain (1 %) at an elevated temperature (220 °C) were performed a priori to monitor the evolution of the storage modulus (G′) of the blends during phase separation. G′ showed almost time independent values after 5 h, manifesting completion of the phase separation process. After 5 h, the blends morphology was characterized in more detail by small amplitude oscillatory measurements as a function of frequency. The strains used were chosen to be within the linear viscoelastic regime.

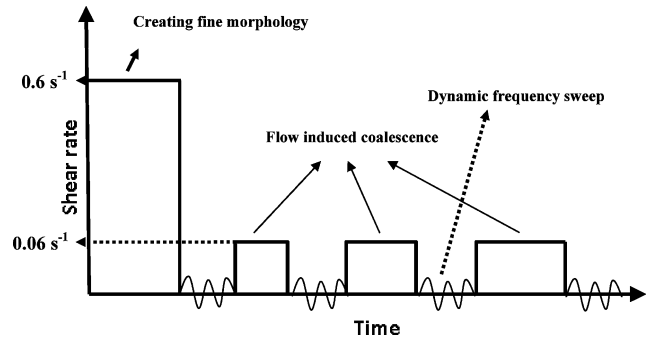

FIGURE 1. Shear protocol used to monitor the flow-induced coalescence.

To investigate the role of NH_2-MWCNTs in stabilizing the PMMA droplets against flow induced coalescence in 85/15 PαMSAN/PMMA blends, a simple shear protocol as a function of time was followed (see Figure 1). The samples were sheared for a fixed duration (1200s) at a shear rate of 0.6 s^{-1}. (This is below the critical shear rate for shear fracture which was determined a priori.) In addition, this shear rate is also located in the region where there is a dynamic equilibrium between coalescence and drop breakup, i.e, above the hysteresis zone. Subsequently, the shear rate was lowered to 0.06 s^{-1}, and coarsening of the morphology is expected due to coalescence. The flow was interrupted from time to time to probe the morphology evolution by measuring linear viscoelastic modulii. The evolution of the interfacial relaxation time or Palierne time ($R\eta_m/\Gamma$; where R is the droplet radius, η_m is the matrix viscosity, and Γ is the interfacial tension between the blend components) was evaluated using the weighted relaxation spectra by the nonlinear regularization (NLREG) method (13).

Dynamic mechanical thermal analysis (DMTA) was performed using Q800 (TA Instruments). The sample dimensions were 17 × 10 × 0.85 mm^3. A tensile force of 0.1 N as preload was applied to the test specimen using a film tension clamp and dynamic frequency of 10 Hz, and 0.05% strain amplitude was applied. Tan δ values were obtained with a temperature ramp of 3 °C/min. The glass transition temperature (T_g) was obtained from the tan δ peaks. It is worth noting that the blends were melt mixed at 190 °C (±2 °C) which is slightly above the cloud point temperature in case of 85/15 PαMSAN/PMMA blends and well above it in case of 15/85 PαMSAN/PMMA blends. Below this temperature, it was not possible to process them due to limitations in the torque values in mini extruder. However, all the samples were compression molded at 160 °C where it is assumed that the squeeze flow deformation during compression molding allows the phase separated regions to mix again or at least transform into microheterogeneous phases. In order to have a quantitative proof of this phenomenon, we monitored the T_g of the compression molded blends. All the blends investigated here indeed exhibited a single T_g confirming the homogeneity of the blends. The tan δ as a function of temperature for 15/85 PαMSAN/PMMA blends is shown as an example (see Figure 2).

Morphological analysis was performed by means of field-emission gun (FEG) scanning electron microscope (SEM, Philips XL30) and transmission electron microscope (TEM, Philips CM 200 FEG). To investigate the morphology of the miscible blends, compression molded samples (pressed at 160 °C) were cryo-fractured in liquid nitrogen and then mounted on the SEM sample holder. The samples were gold sputtered to avoid

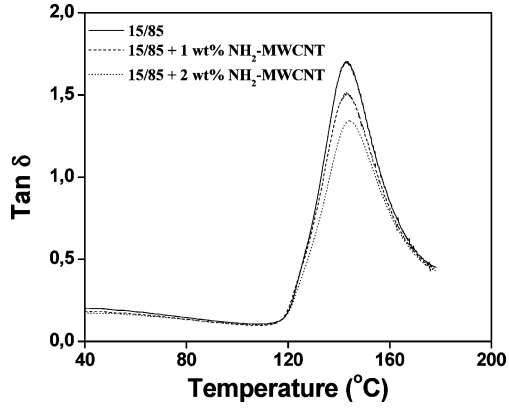

FIGURE 2. Tan δ as a function of temperature for 15/85 PαMSAN/PMMA blends with or without NH_2-MWCNTs.

charging. For TEM, the compression molded samples (pressed at 160 °C) were first annealed at 220 °C for 5 h (to allow complete phase separation) and subsequently quenched to freeze the morphology. The samples were then sectioned by ultramicrotomy to thin lamellae (100 nm) and mounted on a Cu-TEM grid with holey carbon film.

Conductivity spectroscopy measurements were performed both at room temperature and at an elevated temperature (220 °C) on the compression molded samples (16.5 mm diameter and 1.75 mm thickness) in the frequency range of 10^{-2} and 10^7 Hz using a Novocontrol Alpha high resolution dielectric analyzer. The instrument measures the complex impedance of the sample; together, with the knowledge of the geometry of the sample, the complex conductivity is calculated. Further, in this work, the real part of the complex conductivity will be used. For conductivity spectroscopy measurements at elevated temperature (220 °C), the samples were placed between two brass plates, separated by a circular Teflon spacer to maintain a fixed sample geometry in the melt state. The same spacer was used for all the measurements in order to eliminate systematic errors in sample dimensions. The temperature was controlled by a Novocontrol Quatro temperature controller, which uses a nitrogen gas flow to control the sample temperature with an accuracy of 0.1 °C. Frequency scans were performed at a fixed temperature of 220 °C during 5 h. Each frequency scan took about 3 min to complete, 100 such scans were performed. Further details about the dielectric instrumentation and data analysis can be found in refs 14−16. It is also important to note that all the measurements were performed on the compression molded specimens which further reduces any possibility of nanotubes orientation influencing the conductivity of the blends.

3. RESULTS AND DISCUSSION

3.1. Melt Rheology: Percolation and Coalescence Suppression. The interaction between the blend components and the filler is an essential factor in the phase separation processes and the final blend morphology. Hence, it is important to investigate the influence of the NH_2-MWCNTs on the linear viscoelastic behavior of the respective components. For this purpose, composites of PαMSAN/NH_2-MWCNTs and PMMA/NH_2-MWCNTs were prepared with different concentrations of NH_2-MWCNTs under the same extrusion conditions (as described in the Experimental Section). Interconnected structures of anisometric fillers result in a yield stress (17) characterized by the appearance of a plateau in the elastic modulii (G′) at low frequencies. This is an indication of a "sol−gel" transition in the composites due to the formation of a "gel-like" structure by the filler above a critical concentration, a phenomenon usually termed as rheological percolation threshold. This behavior also manifests itself in a divergence of phase angle plotted versus complex modulus ($|G^*|$) in the van Gurp-Palmen plots (18). Figure 3a,b shows that the composites exhibit a "gel-like" behavior for NH_2-MWCNT content above 0.5 wt % in PMMA/NH_2-MWCNT composites and above 2 wt % in PαMSAN/NH_2-MWCNT composites. These differences can be explained on the basis of "specific interactions" of NH_2-MWCNTs with the components. For instance, $-NH_2$ groups on the MWCNT surface can presumably interact with the −O−C═O of PMMA (19) during melt mixing, thus leading to better dispersion.

Figure 3c,d shows the dynamic frequency sweeps of 85/15 and 15/85 PαMSAN/PMMA blends with NH_2-MWCNTs after the complete phase separation (i.e after 5hrs at 220 °C). At low frequencies, the G′ is very sensitive to the morphology. The existence of the dispersed droplet phase is characterized by an increase in the elasticity, manifesting itself in a shoulder in the plot of G′ versus frequency. In addition, G′ at low frequencies tends to a plateau above a critical filler concentration which is a typical solid-like response, manifesting the onset of rheological percolation. In the measured frequency range, such transitions can be seen above 1.25 wt % NH_2-MWCNTs in 85/15 PαMSAN/PMMA blends (see Figure 3c) and above 0.5 wt % NH_2-MWCNTs in 15/85 PαMSAN/PMMA blends (see Figure 3d). It is interesting to note that the rheological percolation threshold in 85/15 PαMSAN/PMMA blends is ∼1.25−1.5 wt % MWCNTs (Figure 3c) as compared to 2 to 3 wt % in PαMSAN/MWNTs composites (Figure 3b) whereas in case of 15/85 PαMSAN/PMMA blends (Figure 3d) the percolation value almost coincides with that of the PMMA/NH_2-MWCNTs system (Figure 3a). It is evident from the linear viscoelastic behavior of the filled components and those of the blends with MWCNTs that the rheological percolation is a complex phenomenon governed by both specific interactions between the filler and the components and the overall state of dispersion of the filler in the blends. In this regard, morphological analysis can provide further insights into the state of dispersion of MWCNTs in the phase separated blends. The latter is discussed in the subsequent sections. Finally, it should be noted that filler concentrations above the percolation threshold could mask the relaxation mechanisms of the droplets which otherwise is clearly visible as a shoulder in G′-frequency curves.

To investigate the role of NH_2-MWCNTs in stabilizing the PMMA droplets against flow-induced coalescence in 85/15 PαMSAN/PMMA blends, a simple shear flow protocol as a function of time was followed (as discussed in the Experimental Section). The dominant relaxation time of the interfacial contribution was determined from the weighted relaxation spectrum obtained after subtracting the component contribution. The evolution of the Palierne time ($R\eta_m/\Gamma$) as a function of time after step-down in shear rate (i.e., coalescence time) is shown in Figure 3e. It is observed that for neat 85/15 PαMSAN/PMMA blends the droplet radius

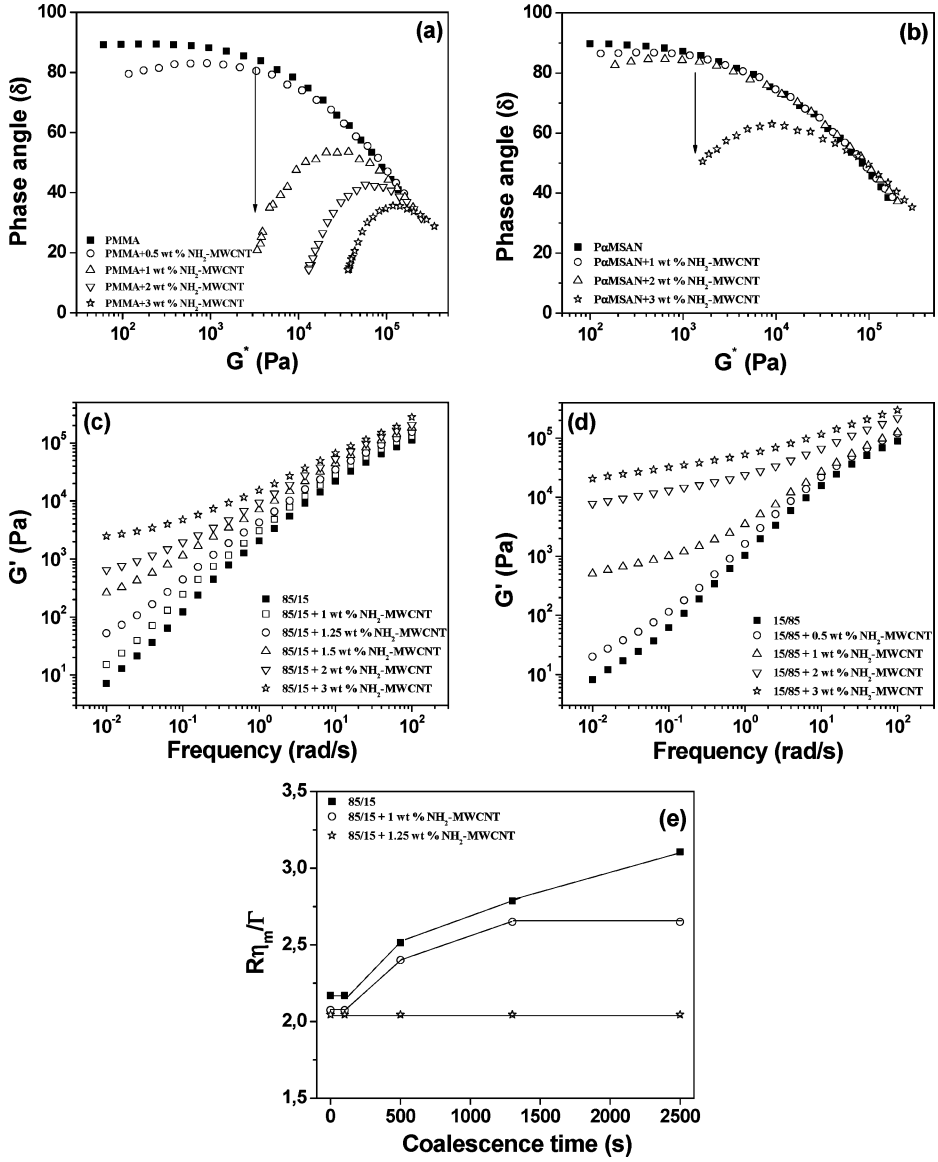

FIGURE 3. van Gurp-Palmen plots for (a) PMMA; (b) PαMSAN with NH_2-MWCNTs; G′ as a function of frequency for (c) 85/15 PαMSAN/PMMA; (d) 15/85 PαMSAN/PMMA blends with NH_2-MWCNTs; (e) Evolution of the interfacial relaxation time ($R\eta_m/\Gamma$) as a function of coalescence time for 85/15 PαMSAN/PMMA blends with or without NH_2-MWCNTs.

increases significantly with time, which is a typical phenomenon of uncompatibilized blends. However, at a loading of 1 wt % NH_2-MWCNTs, the coalescence of the PMMA droplets is slowed down and it is completely suppressed at 1.25 wt % NH_2-MWCNTs in 85/15 PαMSAN/PMMA blends, at least on practical time scales. One comment should be made here regarding the low-frequency plateau modulus. In the present system, we did not observe such phenomenal changes below 1.5 wt % NH_2-MWCNTs (Figure 3c), above which "network-like structure" of MWNTs resulted in a yield stress manifesting itself in a plateau. It was argued (20) that the effects of particle induced "droplet bridging" on the low-frequency plateau modulus and the associated yield stress is small for the system with high viscosities and matrix modulii. (Zero shear viscosities of PαMSAN and PMMA at 220 °C are 10550 Pa s and 6065 Pa s, respectively; $p = 0.6$.) Moreover, the length of NH_2-MWCNTs is on the order of several micrometers, which further reduces the possibility of particle induced "droplet bridging".

3.2. Morphology: Selective Localization of MWCNTs. The role of NH_2-MWCNTs in suppressing coalescence can be elucidated by a detailed morphological analysis. To investigate the state of dispersion of MWCNTs in the miscible blend, FEG-SEM was performed on the compression molded samples. As mentioned in the Experimental Section, all the compression molded blends (pressed at 160 °C) showed a single T_g manifesting the homogeneity of the blends. Figure 4a,b illustrates the cryofractured FEG-SEM images of the miscible blends of 85/15 and 15/85 PαMSAN/PMMA blends with 2 wt % NH_2-MWCNTs, respectively. The sample preparation technique has been described in detail in the Experimental Section. One can clearly observe the random distribution of NH_2-MWCNTs (appearing as white dots representative of the conductive material) in

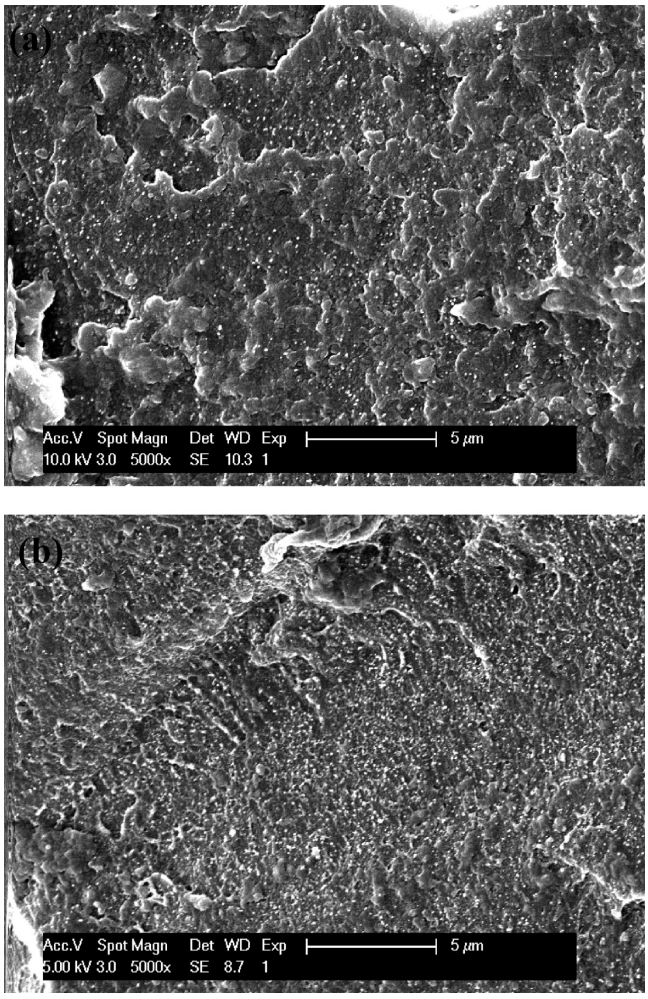

FIGURE 4. FEG-SEM micrographs of miscible blends (compression molded at 160 °C) of PαMSAN/PMMA with 2 wt % NH_2-MWCNTs: (a) 85/15; (b) 15/85.

the homogeneous blends. Figure 5 shows the representative TEM images of the blends after complete phase separation. Figure 5a,b shows the TEM images of a neat 85/15 PαMSAN/PMMA blend (after complete phase separation) and 85/15 blends with 2 wt % NH_2-MWCNTs (after complete phase separation), respectively. The samples were not stained, but the two components (phases) are clearly visible. The matrix component (PαMSAN) appears darker, and the droplets of PMMA appear brighter in the bright-field TEM images. The MWCNTs are relatively well dispersed and are mostly found in the matrix phase with a few located at the interface (see inset of Figure 5b). Knowing that the MWCNTs were randomly distributed before phase separation (see Figure 4), this result clearly shows that the growing PMMA droplets during phase separation allow NH_2-MWCNTs to accumulate in the PαMSAN phase. In this context, it is worth mentioning that the localization of NH_2-MWCNTs in the PαMSAN phase is energetically favored from thermodynamic arguments. In an immiscible polymer blend, the minimization of the interfacial energy is the driving force for the fillers to localize in a specific phase or at the interface (21). A quantitative estimation of wetting coefficient (22) gives an idea about the selective localization of MWCNTs in blends driven by the thermodynamic forces, provided the surface free energy (SFE) of the components, MWCNTs, and the temperature dependency of SFE is known. The SFE of PαMSAN is not readily available in the literature, but on the basis of its chemical structure (70% α-methyl styrene and 30% acrylonitrile), it can be approximated to either α-methyl styrene (γ = 27.4 mN/m at 220 °C, extrapolated from ref 23) or styrene acrylonitrile with 35% acrylonitrile content (SAN, γ = 34.5 mN/m at 220 °C, extrapolated from ref 24, % polarity > 24). The SFE of PMMA is estimated to be 25.9 mN/m at 220 °C; % polarity: 28 (extrapolated from ref 23). The SFE of MWCNTs lies in the range of 27.8−45.3 mN/m (25, 26), depending on the % polarity and the surface chemistry. Both α-methyl styrene and SAN exhibit higher SFE as compared to PMMA at 220 °C. Hence, the localization of MWCNTs can be expected to be energetically favored toward the PαMSAN phase of the blends (i.e., the component having higher SFE). It should also be noted that if the filler has a specific affinity for one of the components in a blend there is little chance for the filler to diffuse to the interface. In addition, localizing MWCNTs at the interface of a polymer blend is quite intricate because their length scales (several micrometers) are often larger than the phase dimensions (for instance, droplet diameter is 100−150 nm in 85/15 blends). Hence, few interactions between $-NH_2$ groups on the MWCNT surface and −O−C═O of PMMA presumably allow some MWCNTs to be present also at the interface (as indicated by arrows in the inset of Figure 5b). However, it should be stressed that the concentration of $-NH_2$ in NH_2-MWCNTs is significantly lower (<0.5%) (11) as compared to the large −O−C═O concentrations in PMMA. Hence, the partial presence of the nanotubes at the interface in 85/15 PαMSAN/PMMA blends can be attributed to the limited interfacial reactions, in the absence of which the localization is thermodynamically more favorable toward the matrix phase (PαMSAN). An optimum concentration of $-NH_2$ functional groups on the MWCNT surface might facilitate more nanotubes to accumulate at the interface. It is interesting to note that, though NH_2-MWCNTs have a specific affinity toward the PαMSAN phase of the blend, they percolate better in the PMMA phase (see Figure 3a,b). This strongly suggests the role of "specific interactions" in governing the rheological percolation threshold. It is, thus, evident from TEM analysis that the relatively well dispersed MWCNTs in the PαMSAN phase and the partial presence of the nanotubes at the interface presumably act as a barrier and suppresses the coalescence of PMMA droplets above a critical concentration (>1 wt %) in 85/15 PαMSAN/PMMA blends.

The TEM image of 15/85 PαMSAN/PMMA blends with 2 wt % NH_2-MWCNTs is shown in figure 5c. The dark regions of figure 5c are the MWCNTs rich PαMSAN domains. As expected, the MWCNTs were preferentially found in the PαMSAN phase of the blend. Rather than a matrix-droplet type morphology, as one would expect, this particular blend showed a highly irregular type of microstructure. More interestingly, the nanotubes are found to bridge the PαMSAN

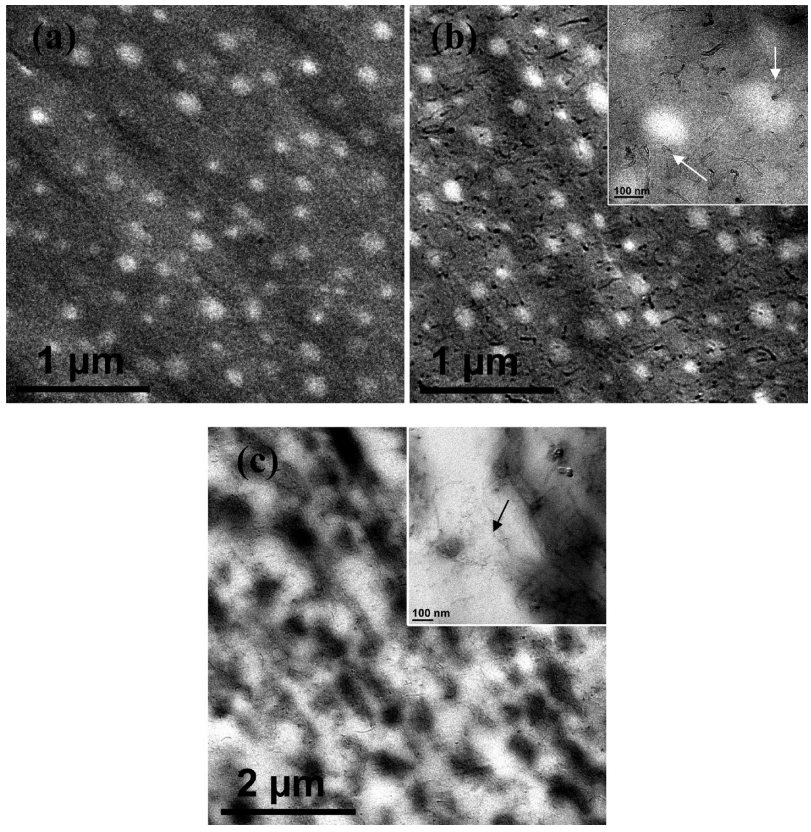

FIGURE 5. TEM images of phase separated PαMSAN/PMMA blends (after annealing at 220 °C for 5 h followed by quenching): (a) neat 85/15; (b) 85/15 with 2 wt % NH_2-MWCNTs (inset showing higher resolution image); (c) 15/85 with 2 wt % NH_2-MWCNTs (inset showing higher resolution image).

domains as evidenced from the higher resolution TEM (see inset of Figure 5c). This could be a possible explanation for the early onset of rheological percolation in 15/85 blends as compared to 85/15 PαMSAN/PMMA blends (see Figures 3c,d). It should be stressed that the MWCNTs were rather randomly distributed in the blends before phase separation and further phase separation led to their selective localization in the PαMSAN phase. This explains the observed lower rheological percolation threshold in phase separated blends (∼1.25−1.5 wt % in 85/15 PαMSAN/PMMA blends and 0.5−1 wt % MWCNTs in 15/85 PαMSAN/PMMA blends) in contrast to the PαMSAN/MWCNTs system (2 to 3 wt % MWCNTs). The heterogeneous distribution resulted in well dispersed MWCNTs rich domains in the blends which will lead to more efficient pathways for percolation.

3.3. Conductivity Spectroscopy: Effect of Heterogeneous Distribution of MWCNTs. Electrical conductivity spectroscopy measurements were performed on the blends with or without NH_2-MWCNTs before phase separation (at room temperature) and during phase separation at an elevated temperature (220 °C) in the melt (Figure 6a). The experimental details of the conductivity spectroscopy at 220 °C are discussed in the Experimental Section. As expected, the neat 85/15 PαMSAN/PMMA blends showed insulating behavior at room temperature and a significant conductivity when phase separated at 220 °C, as indicated by the plateau below a critical frequency (ω_c, 100 Hz) (27). Interestingly, both 85/15 and 15/85 PαMSAN/PMMA blends (the later not shown here for the sake of clarity) with 2 wt

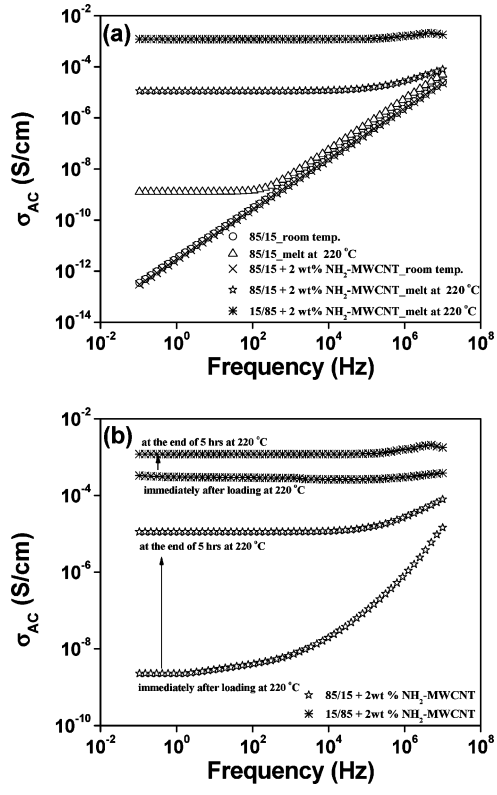

FIGURE 6. Conductivity spectra for 85/15 and 15/85 PαMSAN/PMMA blends with 2 wt % NH_2-MWCNTs: (a) room temperature versus melt; (b) during phase separation.

% NH_2-MWCNTs that showed insulator properties at room temperature (when one phasic) revealed an increase in the conductivity at 220 °C in the melt (when phase separated) by 8 and 10 orders of magnitude, respectively (see Figure 6a). Further, the conductivity spectra showed frequency independent plateau almost in the entire range of frequency, manifesting the formation of percolative "network-like" structure of MWCNTs in the blends. The interconnected domains of NH_2-MWCNTs rich PαMSAN phase presumably resulted in higher conductivity in 15/85 blends as compared to 85/15 PαMSAN/PMMA blends. It is interesting to note that both the set of blends showed insulator properties at room temperature even at 3 wt % MWCNTs (not shown here) whereas substantial increase in the melt-conductivities were observed for the phase separated blends even at lower MWCNT content. These observations are a clear mandate to the fact that NH_2-MWCNTs were randomly distributed in the blends before phase separation and, hence, presumably lacked interconnectivity of the filler. At an elevated temperature, the blends phase separate and allow NH_2-MWCNTs to migrate to the energetically favored phase (PαMSAN) in the blends. This phenomenon is also supported by TEM analysis.

Figure 6b further illustrates these effects by comparing the frequency dependent conductivity spectra of 85/15 and 15/85 PαMSAN/PMMA blends with 2 wt % NH_2-MWCNTs immediately after loading the sample at 220 °C and after 5 h (at 220 °C) which represents complete phase separation. The 85/15 PαMSAN/PMMA blend with 2 wt % NH_2-MWCNTs displays a dramatic increase in conductivity during phase separation, though the final conductivity remains 2 orders of magnitude below that of the 15/85 PαMSAN/PMMA blends. In contrast, the conductivity of 15/85 blends with 2 wt % NH_2-MWCNTs increases marginally after complete phase separation. The conductivity of 15/85 PαMSAN/PMMA blends start at a level being typical for a percolated MWCNT network, a further improvement of the conductivity is obtained upon complete phase separation in contrast to 85/15 blends. The interconnected MWCNTs rich PαMSAN domains in 15/85 PαMSAN/PMMA blends presumably give rise to a higher final electrical conductivity as compared to 85/15 PαMSAN/PMMA blends at a given concentration of MWCNT. Furthermore, the effective increase in the local concentration of MWCNTs in a specific phase facilitated the formation of "network-like" structure. This effective rise in MWCNT concentration in 15/85 blends is by a factor of ~7 as compared to ~1.2 in 85/15 blends (assuming that all the MWCNTs are localized in a specific phase).

Interestingly, despite such a dramatic increase in the local concentration, the melt conductivity is only 2 orders of magnitude higher in 15/85 blends as compared to 85/15 blends and yet reaches only 0.001 % of the bulk conductivity of MWCNTs (assuming bulk conductivity of MWCNTs to be >100 S/cm). At an elevated temperature, dynamic percolation (28) is expected to take place where the filler particles move close to each other and the tunneling resistance (from the insulating polymer layer) is reduced. Above the percolation threshold of MWCNTs, the conducting network develops and spreads gradually in 3D and the conductivity value saturates. Even for a fully percolating CNT network, the conductivity is limited due to CNT-CNT contact resistance (29). CNTs in principle have higher junction resistivity due to smaller CNT-CNT contact surface. A thin layer of insulating polymer can increase the junction resistance and its contribution would be more than for a network of CNTs. Hence, the conductivity values in the composites are far less than the bulk conductivity of neat CNTs. Moreover, the conductivity values saturate above a certain concentration of MWCNTs in the blends investigated here indicating the maximum volume fraction of nanotubes one could achieve in the present system.

Furthermore, the phase separation process can be used as a tool to increase the effective concentration of MWCNTs which otherwise is difficult to process from a practical point of view. It was argued that the polymer chains must be squeezed in order to reduce the surface to surface distance between two CNTs (which is 0.34 nm, also the equilibrium van der Waals' distance) (30). The end to end distance (R) of a flexible polymer chain can be expressed as $R = lN^{0.6}$ where, l is the size of the monomer and N is the number of monomers per polymer chain (31). l is typically larger than 0.154 nm (the C−C bond distance) and assuming N to be 100, $R > 2.44$ nm, which is a factor 7 higher than the equilibrium van der Waals distance. Hence, processing polymer nanocomposites involving higher fractions of MWCNTs becomes practically very difficult. In this context, phase separation of polymer blends can be used as a tool to increase the effective concentrations of MWCNTs. By quenching such morphologies, highly conducting materials with controlled positioning of MWCNTs and phase microstructures can be developed.

Interestingly, it was observed that after a particular time the conductivity values remained almost constant. For the 85/15 PαMSAN/PMMA blends, steady state was reached after approximately 5 h whereas this occurred much earlier in the 15/85 PαMSAN/PMMA blends. These observations can be correlated with the time dependent percolation of MWCNTs in the blends, which is also closely related with temperature and the morphology evolution during phase separation. In the case of 15/85 PαMSAN/PMMA blends, the deeper quench depth above LCST speeded up the phase separation processes. It is evident from Figure 6b that the time required to form percolated "network-like" structure of MWCNTs is significantly lower in the case of 15/85 PαMSAN/PMMA blends as compared to 85/15 PαMSAN/PMMA blends. It has been reported earlier that in phase separating blends with CB the dynamic percolation process is greatly affected by temperature and phase fluctuations (28). Figure 7 further illustrates schematically the use of phase separation as a tool to create controlled dispersion of MWCNTs rich domains in PαMSAN/PMMA blends. Further investigations concerning the kinetics of phase separation of the blends in presence of MWCNTs by conductivity

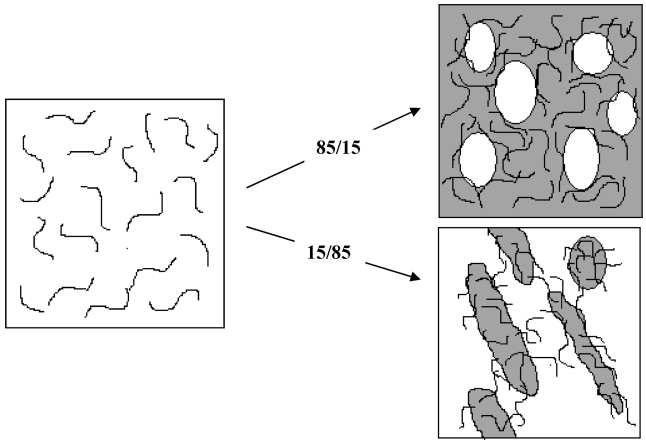

FIGURE 7. Cartoon illustrating the use of phase separation as a tool to create well dispersed MWCNTs rich domains in the blends. (The gray regions indicate the PαMSAN phase; the white regions represent PMMA phase; hairy-like structures represent MWCNTs.)

spectroscopy and time-sweep experiments will be performed in the future.

4. CONCLUSIONS

85/15 and 15/85 PαMSAN/PMMA blends were prepared with or without NH_2-MWCNTs by melt mixing and were allowed to phase separate at elevated temperature (220 °C) in the rheometer. After the complete phase separation process, the morphology of the blends was characterized by rheology, using small amplitude oscillatory measurements as a function of frequency. Further, to investigate the effect of MWCNTs on the flow induced coalescence in 85/15 PαMSAN/PMMA blends, a shear flow protocol was followed. It was found that at a typical loading of 1.25 wt % NH_2-MWCNTs the coalescence of the PMMA droplets was completely suppressed in 85/15 PαMSAN/PMMA blends at least in the practical time scale. Electron microscopic images revealed that the MWCNTs were heterogeneously distributed in the blends as a result of phase separation. This was attributed to the thermodynamically driven migration of NH_2-MWCNTs during phase separation which further led to an increase in their local concentration in a specific phase. Conductivity spectroscopy revealed that the addition of merely 2 wt % NH_2-MWCNTs is able to transform both 85/15 and 15/85 PαMSAN/PMMA blends from virtually insulating at room temperature (one phasic) to a highly conducting material in the melt (two phasic) as a result of phase separation. By quenching such morphologies, a highly conducting material with controlled phase microstructures can be developed. This study clearly shows that the phase separation processes can be used as a tool to create well dispersed MWCNTs in 3D, potentially resulting in more effective percolation as compared to one phasic system. Such materials can be further exploited as soft conductive materials for microstructure controlled electrical devices.

Acknowledgment. Onderzoeksfonds K.U. Leuven (Postdoctoral Fellowship for S.B. and C.Ö.) and Research Foundation-Flanders, FWO (Postdoctoral Fellowship for J.L.) are gratefully acknowledged for financial support. We would also like to thank Mr. Danny Winant, MTM, Katholieke Universiteit Leuven for his kind assistance in dynamic mechanical thermal analysis.

REFERENCES AND NOTES

(1) McMaster, L. P. *Copolymers, Polyblends, and Composite*; Monsanto Co.: Springfield, MA, 1975; Vol. 142, p 43.
(2) Fenouillot, F.; Cassagnau, P.; Majesté, J. *Polymer* **2009**, *50*, 1333.
(3) Harris, P. J. F. *Int. Mater. Rev.* **2004**, *49*, 31.
(4) Bose, S.; Bhattacharyya, A. R.; Bondre, A. P.; Kulkarni, A. R.; Pötschke, P. *J. Polym. Sci., Part B: Polym. Phys.* **2008**, *46*, 1619.
(5) Bose, S.; Bhattacharyya, A. R.; Kulkarni, A. R.; Pötschke, P. *Compos. Sci. Technol.* **2009**, *69*, 365.
(6) Binks, B. P.; Horozov, T. S. *Colloidal Particles at Liquid Interfaces*; Cambridge University Press: Cambridge, U. K., 2006; p 1−74.
(7) Stratford, K.; Adhikari, R.; Pagonabarraga, I.; Desplat, J.-C.; Cates, M. E. *Science* **2005**, *309*, 2198.
(8) Vermant, J.; Cioccolo, G.; Nair, K. G.; Moldenaers, P. *Rheol. Acta* **2004**, *43*, 529.
(9) Gubbels, F.; Jerome, R.; Vanlathem, E.; Deltour, R.; Blacher, S.; Brouers, F. *Chem. Mater.* **1998**, *10*, 1227–35.
(10) Laun, H. M. *Pure App. Chem.* **1998**, *70*, 1547.
(11) http://nanocyl.com.
(12) Chae, H. G.; Liu, J.; Kumar, S. In *Carbon Nanotubes: Properties and Applications*, O'Connell, M. J., Ed.; CRC Press (Taylor and Francis group): Florida, 2006; Chapter 8, p 215.
(13) Yu, W.; Bousmina., M.; Zhou, C. *J. Non-Newtonian Fluid Mech.* **2006**, *133*, 57.
(14) Alig, I.; Lellinger, D.; Dudkin, S. M.; Pötschke, P. *Polymer* **2007**, *48*, 1020.
(15) Serwadczak, M.; Wübbenhorst, M.; Kucharski, S. *J. Non-Cryst. Solids* **2007**, *353*, 4303.
(16) Wübbenhorst, M.; van Turnhout, J. *J. Non-Cryst. Solids* **2002**, *305*, 40.
(17) Utracki, L. A. *Polym. Compos.* **1986**, *7*, 274.
(18) van Gurp, M.; Palmen, J. *Rheol. Bull.* **1998**, *67*, 5.
(19) Zhang, K.; Lim, J. Y.; Choi, H. J. *Diamond Relat. Mater.* **2009**, *18*, 316.
(20) Vermant, J.; Vanderbril, S.; Dewitte, C.; Moldenaers, P. *Rheol. Acta* **2008**, *47*, 835.
(21) Ko, S. W.; Hong, M. K.; Park, B. J.; Gupta, R. K.; Choi, H. J.; Bhattacharya, S. N. *Polym. Bull.* **2009**, *63*, 125.
(22) Sumita, M.; Sakata, K.; Asai, S.; Miyasaka, K.; Nakagawa, H. *Polym. Bull.* **1991**, *25*, 265.
(23) http://www.surface-tension.de/solid-surface-energy.htm.
(24) Pionteck, J.; Kressler, J. *The European Physical Society*; Europhysics Conference Abstracts: Mulhouse, France, 1997; p 31.
(25) Nuriel, S.; Liu, L.; Barber, A. H.; Wagner, H. D. *Chem. Phys. Lett.* **2005**, *404*, 263.
(26) Barber, A. H.; Cohen, S. R.; Wagner, H. D. *Phys. Rev. Lett.* **2004**, *92*, 186103.
(27) Leys, J.; Wübbenhorst, M.; Menon, C. P.; Rajesh, R.; Thoen, J.; Glorieux, C.; Nockemann, P.; Thijs, B.; Binnemans, K.; Longuemart, S. *J. Chem. Phys.* **2008**, *128*, 064509(1−7).
(28) Wu, G.; Miura, T.; Asai, S.; Sumita, M. *Polymer* **2001**, *42*, 3271.
(29) Yao, Z.; Kane, C. L.; Dekker, C. *Phys. Rev. Lett.* **2000**, *84*, 2941.
(30) Jiang, B.; Liu, C.; Zhang, C.; Liang, R.; Wang, B. *Composites, Part B* **2009**, *40*, 212.
(31) Flory, P. J. *Principles of Polymer Chemistry*; Cornell University Press: Ithaca, NY, 1953.

AM9008067